ASCE National Structural Engineering Meeting

April 9 - 13, 1973 - San Francisco, California

SIMULATED EARTHQUAKE TESTS OF R/C FRAMES

Shunsuke Otani, A. M. ASCE and
Mete A. Sozen, M. ASCE

Meeting Preprint 1976

SIMULATED EARTHQUAKE TESTS OF R/C FRAMES

by Shunsuke Otani[1], A.M. ASCE and Mete A. Sozen[2], M.ASCE

INTRODUCTION

The inelastic dynamic response of reinforced concrete frames was investigated by subjecting a series of one-bay three-story small-scale structures to strong base motions simulating one horizontal component of representative earthquake acceleration records. The results were studied using linear and nonlinear analysis techniques (1).

This paper evaluates the test results from the perspective of analytical methods routinely and economically available to structural-design offices: linear dynamic response analysis and static limit analysis based on elasto-plastic response.

The experimental program included three test structures (Fig. 1-3). Each structure was subjected to a series of test runs of increasing intensity.

TEST STRUCTURES

A test structure (Fig. 3) consisted of two identical frames, fastened to the earthquake simulator platform, parallel to each other and to the direction of motion. The two frames were connected at each beam level by rigid steel racks carrying steel weights such that the total effective floor weight was 1960 lb. The racks connected with brackets (Fig. 1) outside the frame joints.

---

[1]Research Associate in Civil Engineering, University of Illinois at Urbana-Champaign, Illinois.

[2]Professor of Civil Engineering, University of Illinois at Urbana-Champaign, Illinois.

The dimensions of a typical frame and the arrangement of reinforcement are shown in Fig. 1. The dimensions of beam and column sections are listed in Fig. 2. Gross total longitudinal reinforcement ratios were 0.027 for the beams and 0.032 for the columns.

The first two structures D1 and D2 were identically designed. Structure D3 was designed to have 95 and 90 percent of the yield moments for the columns and the beams, respectively, of the first two structures.

Small-aggregate concrete with high-early-strength cement (Type III), fine lake sand, and Wabash River sand (a mix ratio of 1:1:4 by dry weight) were used in casting all the frames with a nominal water cement ratio of 0.7. The average compressive strength, tensile strength from splitting tests, and secant modulus at 40 percent of the compressive strength were 5,050 psi, 430 psi and 3.16×10^6 psi, respectively, determined by 4 by 8-in. cylinder tests.

No. 2 deformed bars were used as longitudinal reinforcement in the columns and beams, and No. 3 deformed bars in the base girders. Number 14 gage plain wires were used as stirrup reinforcement. Properties of the steel are listed in Table 1.

The longitudinal reinforcement in the beams and columns was provided with sufficient anchorage length either outside the beam-column joints or in the base girder. All frame members and joints, were provided with sufficient web reinforcement.

INSTRUMENTATION

Deformation of the test frames in the direction of motion was measured by differential transformers (LVDT) at each beam level relative to the base girder. Absolute accelerations at each beam level and on the base

girder were measured by servo-accelerometers with a flat response range of 0 to 100 Hz.

The signals from all sensors were continuously recorded on magnetic tape and were digitized later at 2-msec intervals. Base shear and moment signals were computed for a single frame from the synchronized digitized acceleration signals at the three levels, the floor weights, and the story heights. The overturning effect of gravity loads acting through the sidesway displacement (the P-Δ effect) was ignored in calculating base shears and moments.

STRUCTURAL PROPERTIES

Member Stiffness. Moment-curvature relationships of the frame members were calculated from the geometry of the section, and the properties of concrete and reinforcing steel. It was assumed that the strain distribution over the depth of the section was linear and that column axial loads were those due to gravity. Moments and curvatures are listed in Table 2, corresponding to tensile cracking of the concrete, yielding of the tensile steel, and the extreme compressive fiber strain reaching a limiting concrete strain of 0.004. The moment-load-curvature interaction diagram for a column in structures D1 and D2 is shown in Fig. 4.

The stiffness of the members was evaluated for (a) "uncracked" sections and (b) "cracked" sections. Flexural stiffness of "uncracked" sections was defined by the slope of a moment-curvature curve before tensile cracking of the concrete. Flexural stiffness of "cracked" sections was defined by the slope of a line between the origin and a point corresponding to yielding of the tensile reinforcement in the moment-curvature diagram.

Modal Analysis. Each frame was analyzed as a plane frame fixed at the base with massless elastic prismatic members, each of which was represented by its centroidal axis between adjacent beam-column joints. Only flexural deformation was considered. All masses were concentrated at the beam-column joints. Each specimen was idealized into a three-degree-of-freedom system.

Calculated modal frequencies and mode shape vectors for the three modes of vibration are listed in Table 3. The listed mode shape vectors include the corresponding participation factors. Modal responses of a single frame due to a 1.0g spectral acceleration response are plotted in Fig. 5 to show the probable modal contribution to the response of the frame for a 1.0g spectral acceleration response.

Limit Analysis. An elasto-plastic limit analysis was carried out for the idealized frame model using yield moments of the members as listed in Table 2 and "cracked" stiffness. The frame was subjected to either (a) equal loads (uniform load distribution) at the three levels, or (b) loads proportional to the height of each level from the base (triangular load distribution). Base shears (single frame) corresponding to three modes mechanisms are shown in Fig. 6. Mechanism (b) requires the least base shear for both uniform and triangular load distributions.

Dynamic Analysis. Linearly elastic response ("elastic response") of the test structures to measured base motions was calculated by a step-by-step numerical method. Acceleration was assumed to vary linearly over time intervals of 2 msec. Damping factors for the first three modes were assumed to be 5.0, 5.0 and 7.4 percent of critical. The stiffness of the structure was evaluated for both "uncracked" and "cracked" sections.

BASE MOTIONS

The motion of the earthquake simulator platform (2) was programmed to reproduce the acceleration waveform pattern of either the NS component of the 1940 El Centro record (the Imperial Valley Earthquake), referred to as El Centro, or the N21E component of the 1952 Taft record (the Kern County Earthquake), referred to as Taft.

To obtain a representative relation between the vibration frequencies of the specimens and the frequency content of the base motion, the time axis of the earthquake records was compressed by a factor of 2.5. Base-motion amplitudes were chosen arbitrarily, and were increased stepwise in successive test runs up to the capacity of the earthquake simulator. The earthquake simulator (2) could reproduce, within the range of structural engineering interest, scaled acceleration histories with characteristics quite similar to those of the input earthquake records.

It was necessary to find an index to define the intensity of base motion in order to compare and evaluate the effect of different base motions on the behavior of the test structures. The maximum base acceleration was not found to be a good index due to the fact that the maximum acceleration amplitude was easily affected by the existence of accidental high frequency signals.

The spectral intensity (3) at a 20 percent of critical damping factor was adopted in this study to define the intensity of base motion. The range of periods of 0.04 to 1.0 sec was used so as to be consistent with the time scale of 1/2.5 in the tests.

Typical response spectra are shown in Fig. 7 for simulated El Centro and Taft base acceleration signals.

TEST RESULTS

Introduction. All three specimens withstood, without collapse, the base motions of maximum accelerations ranging from 0.24 to 3.4g, or from 0.4 to 5.7 times the base shear coefficient calculated from limit analysis at the formation of collapse mechanism. The maximum first level displacement was measured to be as large as one-twentieth of the first-story height.

Wide cracks were observed at the base of the first-story columns, at the top of the second-story columns, and at the ends of the first- and second-level beams. Diagonal X-shaped cracks were formed in the first- and second-level "joint cores."

The observed heavy damage was limited to the base of the first-story columns. All damage was attributable to axial load and/or flexure without complications due to shear and bond stresses.

Response Waveform. A set of typical observed response waveforms are shown in Fig. 8. The El Centro motion was simulated in the first test run of structure D2 with a spectrum intensity of 15.8 in. and maximum base acceleration of 0.86g.

General observations about the measured waveforms are:

(a) Acceleration waveforms contained more of "higher mode" components, especially at the lower levels. As the intensity of base motion was increased, the "higher mode" components became more perceptible even in the third level waveform, in which the "first mode" component had prevailed.

(b) Displacement waveforms were very smooth at the three levels, dominated by the "first mode" component. The effect of the "higher mode" components, however, became noticeable as the intensity of base motion increased.

(c) Base shear and overturning moment waveforms were governed by the "first mode" component. The influence of the "higher mode" components was larger in the base shear waveform than in the base moment waveform.

Vibration Mode. The terms "first mode" and "higher modes" were used to describe the phase relationship of the three signals, "first mode" implies that all three level signals oscillated in the same phase. "Second mode" implies that only two adjacent level signals were in the same phase. "Third mode" implies that the first- and third-level signals were in phase.

Existence of certain frequencies associated with these three modes was observed on the response signal traces, although the frequencies changed evidently related to the amount of structural damage. The existence of such frequencies and the phase relations can be best demonstrated by examining a smooth base shear waveform (Fig. 8), obtained as the algebraic sum of products of acceleration amplitudes and corresponding masses. For the sum to be smooth, acceleration signals at the three levels should contain common higher frequency components with at least one signal out of phase. The usage of the terms is consistent with the vibration modes associated with a linearly elastic system.

Frequencies. Frequencies associated with each mode of vibration were determined by measuring the average period of three to ten cycles of clearly identified oscillations. The first mode frequency was usually found on displacement signal traces, and the second- and third-mode frequencies on acceleration signal traces.

The ratios of the measured lowest frequencies of each mode in a test run to the calculated elastic modal frequencies (uncracked stiffness in Table 3) are shown in Fig. 9. A free vibration test before Test D1 indicated a frequency approximately 80 percent of the calculated frequency for the first

and second modes. The measured frequencies changed drastically during the first test run. The first-mode frequency at the end of the last test run was reduced to a quarter of the calculated frequency.

Maximum Response. Maximum amplitudes of the measured response signals, automatically picked up during the data reduction process, are compared with spectrum intensity in Fig. 10.

The accelerations increased with spectrum intensities up to a spectrum intensity of approximately 10 in. After that the rate of increase in the accelerations slowed down due to "yielding" of the members. The fact that structure D3 was weaker than D1 and D2 did not show up in the plots.

Total displacement ranges, which are the sum of positive and negative extreme displacements, increased almost linearly with spectrum intensity. Structure D3 had larger displacements at the three levels than D1 and D2.

The total displacement range rather than the absolute maximum displacement was used as a damage index because the absolute maximum displacement was affected by the location of the zero axis, which could shift between test runs due to a temperature change in electronic devices or to an accidental shock applied to the specimen, while the total displacement range was independent of the location of the zero axis.

Maximum base shears and moments increased linearly with spectrum intensity up to a spectrum intensity of approximately 10.0 in., and then appeared to reach a plateau at a base shear of approximately 2. 8 kip and a base moment of approximately 110 kip-in.

DISCUSSION OF THE TEST RESULTS

The test results were evaluated from the viewpoint of methods routinely available to design offices: linearly elastic dynamic and elasto-plastic static limit analyses. Although the results of the response-history analysis are given in this paper, it should be noted that the square root of the sum of the squares of the maximum modal components (4) led to almost identical accelerations, and that the maximum first-mode components provided good approximations to displacements, base shear and base overturning moments of the elastic system. Measured initial frequencies of the specimens were approximately 80 percent of the frequencies calculated for "uncracked" stiffness, and 115 percent of the ones calculated for "cracked" stiffness. Unavoidable cracks were formed in addition to shrinkage cracks in the beam-column connections when the heavy steel racks were secured to the test frames. The measured initial frequencies, which were lower than the calculated values, might have been attributable to the existence of these fine cracks before the test run.

Wide cracks were observed in the same locations as yielding was predicted by the limit analysis for the collapse mechanism.

Acceleration Response. Figure 11a shows that accelerations calculated at the three levels for cracked and uncracked sections were comparable and that the measured values deviated from those calculated at spectrum intensities exceeding 7.0 in. for the third level and approximately 10.0 in. for the other levels.

The deviation could be anticipated by comparing the calculated base shear (Fig. 11c) with the base shear for the collapse mechanism (Fig. 6). However, linear-response calculations would be of no direct use in estimating the accelerations of the three levels.

Linear response analysis does provide a clue to the observed acceleration waveforms. Initially the spectral accelerations for the three modes were comparable, and acceleration waveforms were expected to contain higher mode components, especially at the lower levels, as shown in Fig. 8. However, as the structural stiffness decreased in successive test runs, the fundamental frequency shifted from the "constant-acceleration" to the "constant-velocity" range of the idealized spectral response curve. Thus, the first mode responses made relatively smaller contributions to the overall response as the base-motion intensity was increased.

Displacement Response. The smoothness of the displacement waveforms (Fig. 8) may be mainly attributable to the ratios of the modal spectral responses: the first-mode component (at level 3) for both stiffness assumptions was approximately 10 times as large as the second- and 30 times as large as the third-mode components.

For displacements based on cracked section, there was apparent agreement with measurements at level 3 and poor agreement at level 1 (Fig. 11b). Calculations based on a lower damping value would have reversed the comparison.

Taking the first-level displacement as unity, the measured maximum displacements varied approximately as 1.0:1.9:2.3(D1), 1.0:1.9:2.7(D2) and 1.0:1.7:2.1(D3), while the calculated deflections vary as the first-mode vector (1.0:2.6:3.6) which dominates. Therefore, linear-response calculations could not be used to determine deflections at all three levels. It is of interest to note that the calculated deflections varied as 1.0:2.0:2.6 at the formation of an elasto-plastic collapse mechanism for story lateral loads varying proportionally with height.

Base-shear Response. Figure 11c compares the measured and calculated base shears. A salient feature of the measured base shear is that it has exceeded the value of 1.73 kips indicated by elasto-plastic analysis. This is due to the strain-hardening properties of the reinforcement. Figure 10c shows the limit of 3.3 kips to the base shear obtained by assuming a mechanism forming in the first story only (yielding top and bottom of columns) with the maximum moments based on the strength of the reinforcement. No measurements exceeded this limit, but the data were closer to this limit than the lower bound limit obtained by elasto-plastic analysis.

As would be expected, the base shear from linear response analysis deviates from the measured values at the onset of inelastic response which occurs at a low spectrum intensity. Because the base shear is a key design parameter, it merits further discussion to consider whether the calculated base shear can be reconciled with the measured value on the basis of references to damping and ductility. In describing this process, it is necessary to set up a strawman because the exact use of these concepts in design is not precisely defined. Let the attained ductility, μ, of the test structure be the ratio of the attained displacement (in a particular test run) to the yield displacement at the first level, the latter value being the calculated displacement for the base shear at collapse (elasto-plastic response) on the basis of the cracked-section stiffness.

Figure 12 shows the ratio, γ, of the maximum calculated elastic base shear (for cracked section and damping factors of 0.02, 0.05, and 0.10) to the measured maximum base shear as a function of the attained ductility. Line A represents $\gamma = \mu$ while line B represents $\gamma=\sqrt{2\mu-1}$. The plotted points refer to values of γ and μ obtained from measured values of base shear and maximum displacement at first level. For a given attained ductility, μ, the curves

indicate the expected value of γ while the points indicate the attained value.

A comparison of the data with curves A and B indicates that, with ductility defined as above, curve B and the data can be reconciled for a damping factor of 0.02. Also, even curve A could be reconciled to the data by assuming a lower damping factor. However, reconciliation cannot be obtained with either curve with damping factors higher than 0.02. It would be possible to obtain acceptable reconciliation for any of the cases shown in Fig. 12 by suitable definitions of the yield deflection. However, the use of such an approach as a general design method for multistory frames is not justifiable on the basis of the available evidence.

Base Overturning Moments. Overturning moments at the base of the test frame was calculated as the algebraic sum of the products of lateral forces and corresponding height of the levels from the base. As would be expected from the modal overturning moment response (Fig. 5), the base moment waveforms were almost exclusively governed by the first mode component.

Measured maximum base moments are compared with calculated maximum base moments in Fig. 11d. Similar to the comparison of base shears, calculated elastic base moments (based on both uncracked and cracked stiffnesses) agreed well with the measured values up to a spectrum intensity of 7 in.

The base moment calculated at the formation of the collapse mechanism under a triangular load distribution was approximately 70 kip-in., a value which was exceeded by the measured base moment (Fig. 10) after a spectrum intensity of 7 in.

A limiting value of base moment for a single test frame with elasto-plastic member characteristics can be calculated assuming yield moments at the ends of the three beams, and at the bases of the first-story columns, and

using the clear length of each member. Then overturning moment at the base became 80 kip-in., a value of which was clearly exceeded by the measured base moment after a spectrum intensity reached 15 in.

If moments corresponding to the ultimate stress of the tensile reinforcement were assumed at the same locations, the limiting value of base motion were calculated to be 121 kip-in., which caused a net tensile force of 1.2 kips in a first-story column. The measured base moments were mostly less than this limiting value. The measured maximum overturning moments above 73 kip-in. must have given rise to net tensile stress in the tension side column during the tests.

CONCLUSIONS

1. The test frames resisted the severe base motions without collapse. This observation should be qualified by two considerations: (a) The columns had continuous longitudinal reinforcement and sufficient web reinforcement was provided in the frame members and joints. (b) The maximum story drift reached approximately five percent of the story height.

2. The maximum base shears and overturning moments were approximately 1.7 times the values based on elasto-plastic limit analysis. Strain-hardening characteristics of the reinforcing steel must be explicitly considered in the earthquake-resistant design of reinforced concrete structures, especially in relation to design of web reinforcement, foundations, and columns.

3. Linear dynamic analyses of the test structures provided a good qualitative understanding of the observed inelastic behavior. In predicting a quantitative response of a reinforced concrete system, linear analysis is handicapped not only by the possible yielding of the structure but also by the drastic changes in stiffness which occur due to progressive cracking.

ACKNOWLEDGMENT

The reported work was carried out at the Structural Research Laboratory of the University of Illinois under NSF Grant GI30760X.

Acknowledgment is due to V. J. McDonald, Associate Professor of Civil Engineering, and P. B. Waller, M. Swatta, E. Hanson, and J. K. Wight, graduate research assistants, for their contributions to the execution of the tests. The IBM 360/75 computer system of the Department of Computer Science was used for the computations included in this report.

APPENDIX I. REFERENCES

1. Otani, S. and M. A. Sozen, "Behavior of Multistory Reinforced Concrete Frames During Earthquakes," Civil Engineering Studies, Structural Research Series No. 392, University of Illinois, Urbana, November 1972.

2. Sozen, M. A., and S. Otani, "Performance of the University of Illinois Earthquake Simulator in Reproducing Scaled Earthquake Motions," Proc. U.S.-Japan Seminar on Earthquake Engineering with Emphasis on the Safety of School Buildings, Sendai, September, 1970, pp. 278-302.

3. Housner, G. W., "Spectrum Intensities of Strong Motion Earthquakes," Proc., 1952 Symposium on Earthquake and Blast Effects on Structures, Earthquake Engineering Research Institute, 1952.

4. Rosenblueth, E., "A Basis for Aseismic Design," thesis submitted to the University of Illinois in partial fulfillment of the requirements of the degree of Doctor of Philosophy in Civil Engineering, 1951.

APPENDIX II. NOTATION

The following symbols are used in this paper:

E_s = modulus of elasticity of steel (=29,000,000 psi)

M = bending moment

SI_{20} = spectrum intensity at a damping factor of 0.20

β = damping factor for the first mode

γ = base shear reduction factor

ε_{cu} = assumed limiting strain of concrete (=0.004)

ϕ = curvatures

μ = attained ductility factor at the first level

Table 1. PROPERTIES OF REINFORCING STEEL

Reinforcing Bars	Nominal Area (in^2)	Yield Stress (psi)	Ultimate Stress (psi)
No. 2 Bar	0.050	42,600	66,500
No. 3 Bar	0.11	47,500	71,600
No. 14 gage wire	0.0050	39,600	54,400

Young's modulus E_s = 29,000,000 psi

Table 2. MOMENT-CURVATURE RELATIONSHIPS OF THE MEMBERS

Member	Cracking		Yielding		e_{cu}=0.004	
	M	Ø	M	Ø	M	Ø
(a)Specimens D1 and D2						
First Story Column	2.51	0.176	9.01	1.215	9.56	9.20
Second Story Column	2.24	0.157	8.59	1.185	9.15	9.50
Third Story Column	1.97	0.138	8.16	1.151	8.78	9.80
Beams	2.38	0.0992	9.67	0.875	10.81	9.60
(b)Specimen D3						
First Story Column	2.11	0.160	8.55	1.289	9.13	8.00
Second Story Column	1.84	0.140	8.16	1.254	8.72	8.26
Third Story Column	1.56	0.119	7.75	1.223	8.32	8.57
Beams	1.76	0.0815	8.86	0.967	9.72	7.61

M = moment, kip-in.

Ø = curvature, $\times 10^{-3}$ 1/in.

e_{cu} = assumed limiting strain of concrete in compression

Table 3. CALCULATED FREQUENCIES AND MODE SHAPE VECTORS

(a)Frequencies, Hz Mode	Uncracked Section D1, D2	Uncracked Section D3	Cracked Section D1, D2	Cracked Section D3
First Mode	7.2	7.1	5.0	4.7
Second Mode	23.8	23.3	16.7	15.6
Third Mode	41.5	40.8	29.5	27.9

(b)Mode Shape Vectors

Level	First Mode	Second Mode	Third Mode
3	1.256	-0.341	0.086
2	0.893	0.332	-0.226
1	0.345	0.382	0.273

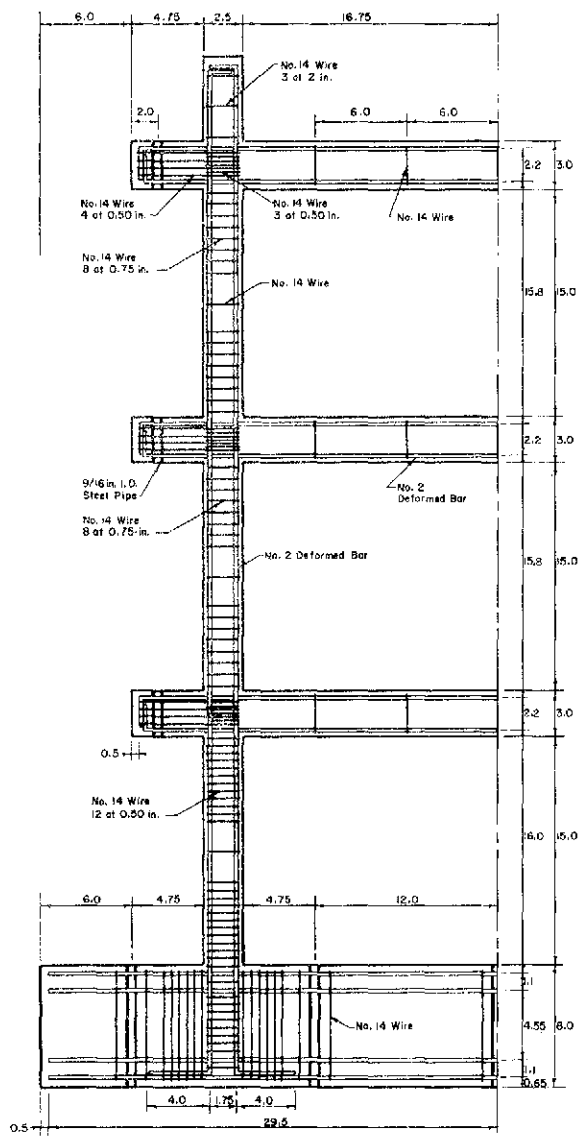

FIG. 1 TEST FRAMES

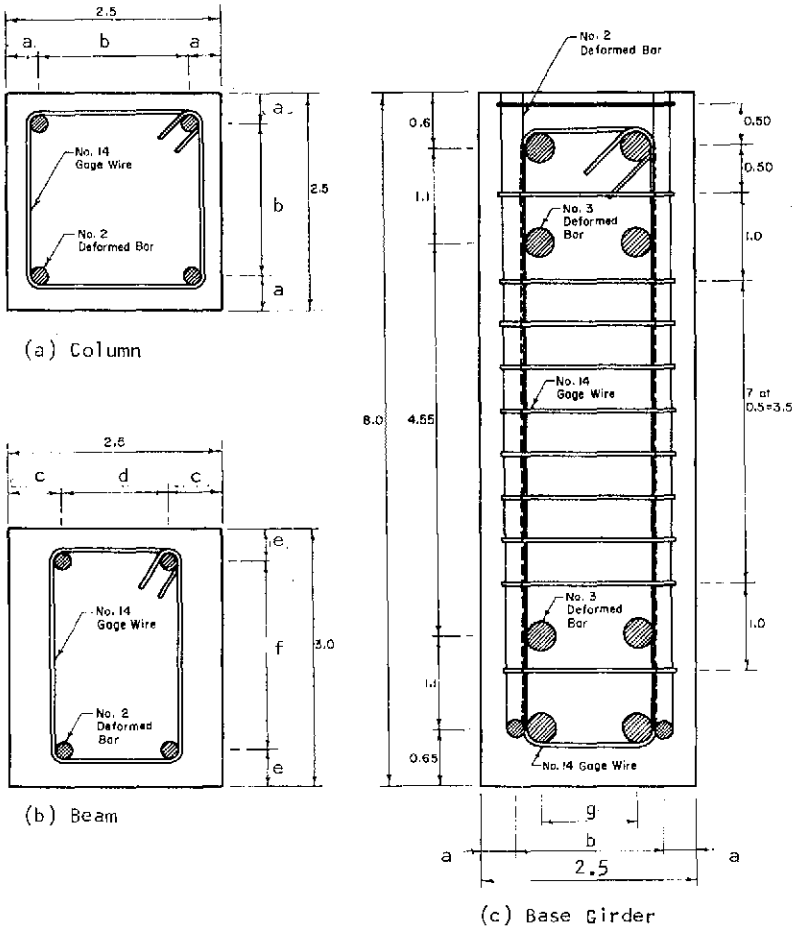

STRUCTURES	a	b	c	d	e	f	g
D1, D2	0.38	1.75	0.63	1.25	0.40	2.2	1.10
D3	0.45	1.60	0.70	1.10	0.55	1.9	0.95

Dimensions in in.

FIG. 2 BEAM AND COLUMN SECTION

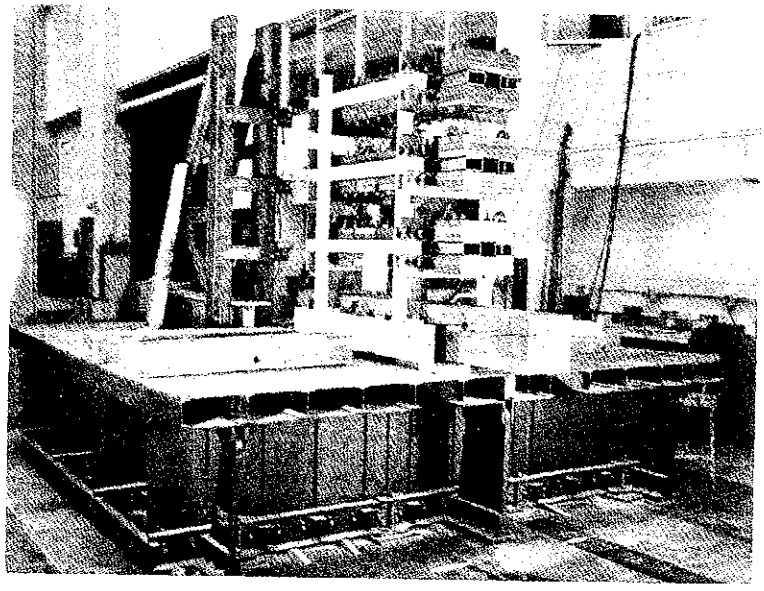

FIG. 3 TEST STRUCTURE ON PLATFORM OF EARTHQUAKE SIMULATOR

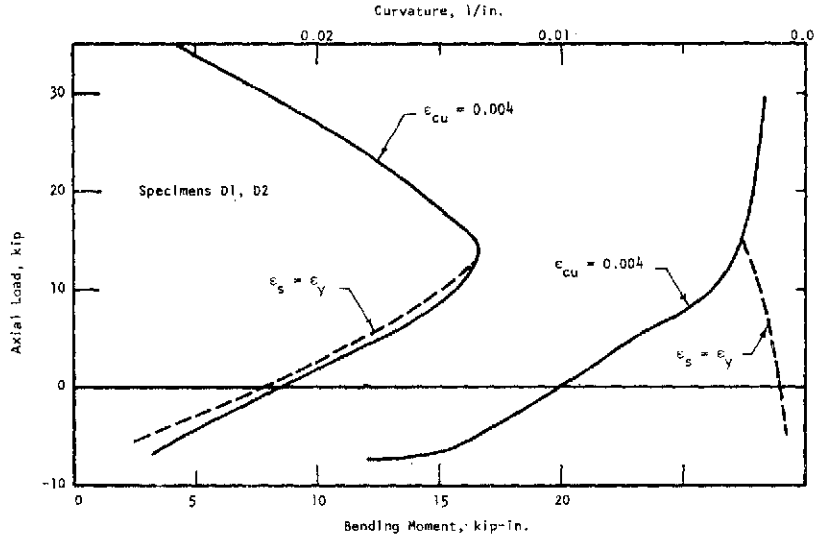

FIG. 4 TYPICAL INTERACTION DIAGRAM FOR COLUMN SECTION (STRUCTURES D1 and D2)

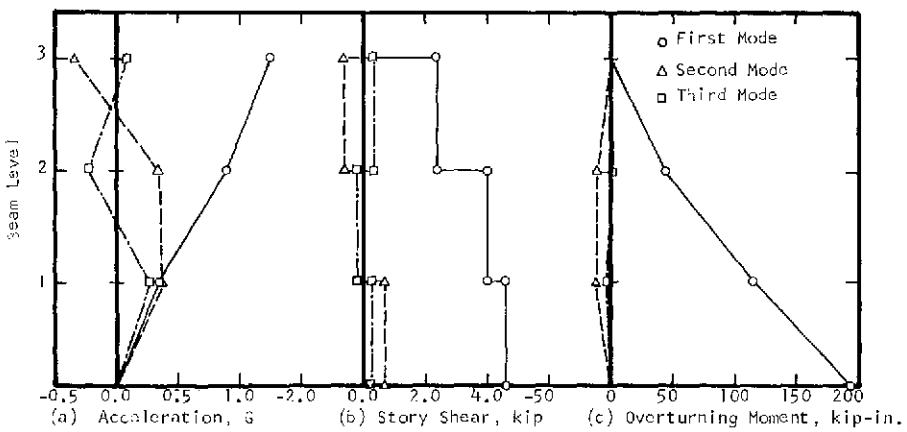

FIG. 5 MODAL ACCELERATION, STORY SHEAR, AND OVERTURNING MOMENT DUE TO 1.0g SPECTRAL RESPONSE

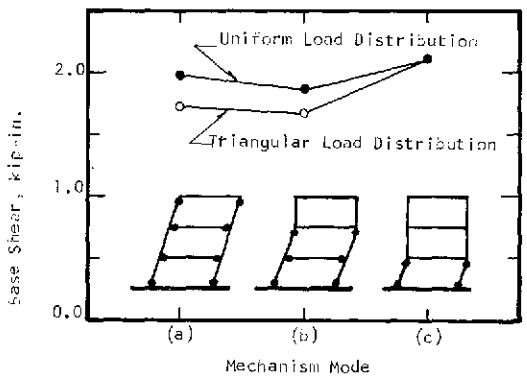

FIG. 6 BASE SHEARS FOR COLLAPSE MECHANISMS UNDER DIFFERENT DISTRIBUTIONS OF LATERAL LOAD AT BEAM LEVEL

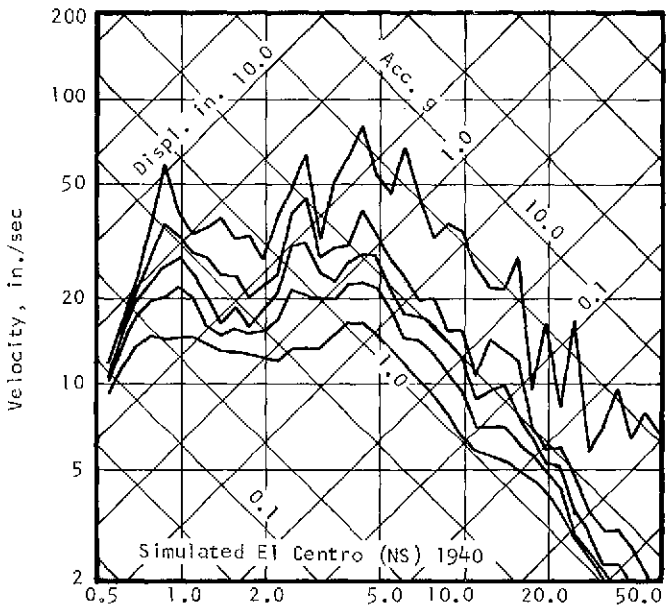

(a) Test D2-1, SI_{20} = 15.8 in.

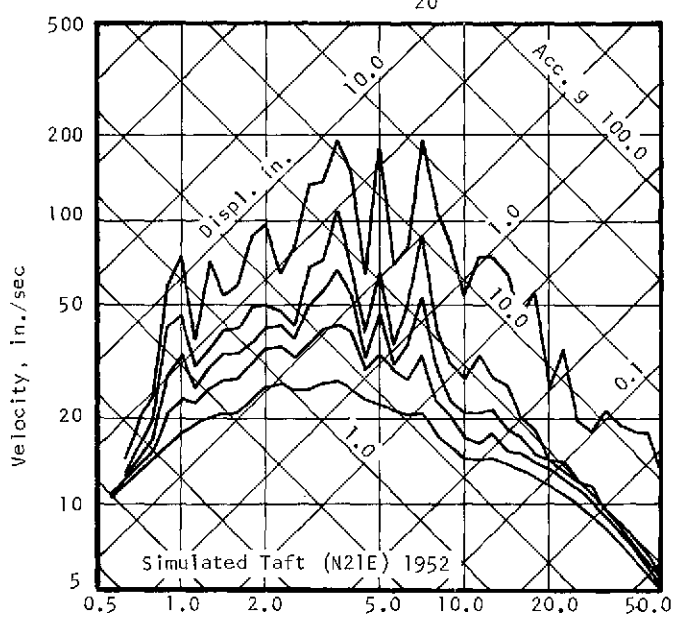

(b) Test D2-4, SI_{20} = 28.4 in.

FIG. 7 TYPICAL RESPONSE SPECTRA FOR MEASURED BASE MOTIONS (β = 0.0, 0.02, 0.05, 0.10, 0.20)

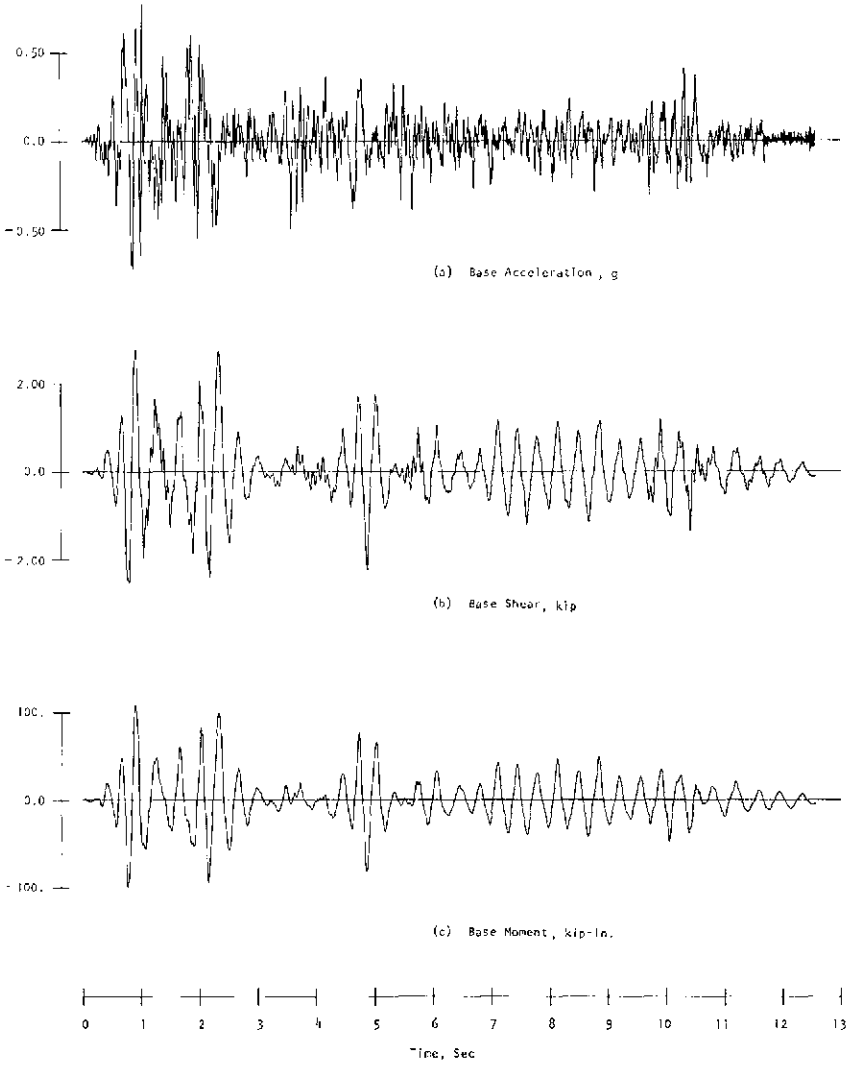

FIG. 8 TYPICAL OBSERVED RESPONSE (TEST D2-1, BASED ON EL CENTRO 1940 NS, SI_{20} = 15.8 in.)

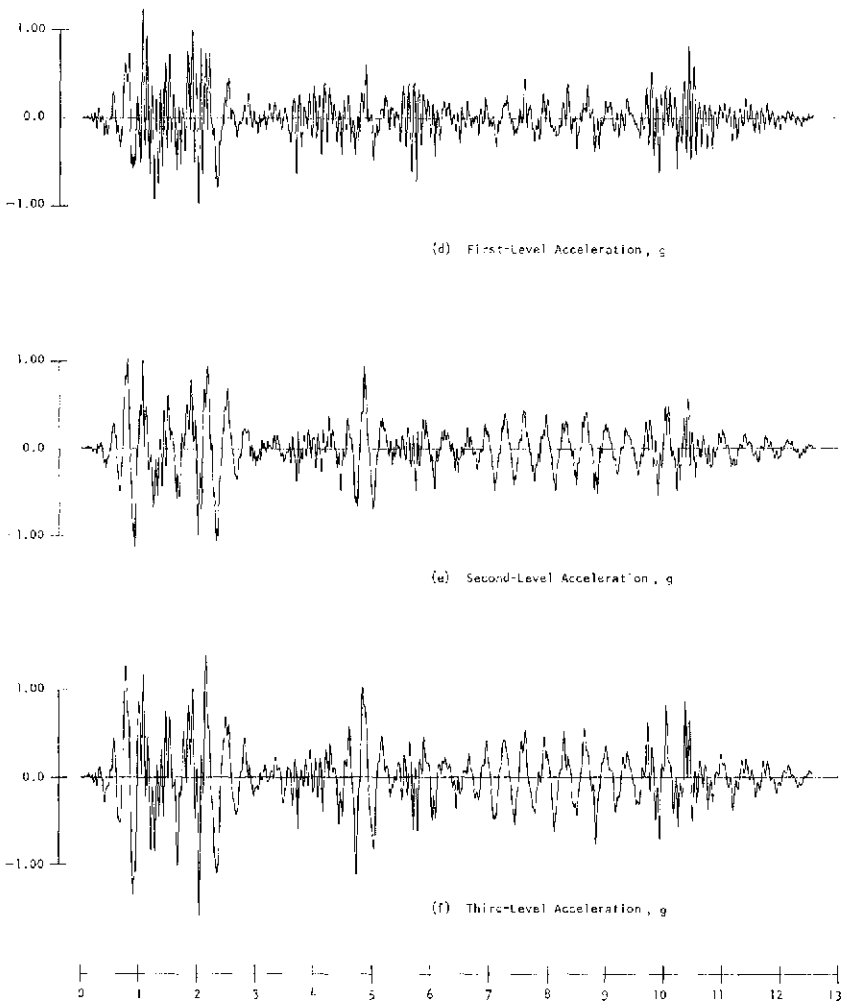

FIG. 8 (Cont'd) TYPICAL OBSERVED RESPONSE (TEST D2-1, BASED ON EL CENTRO 1940 NS, SI_{20} = 15.8 in.)

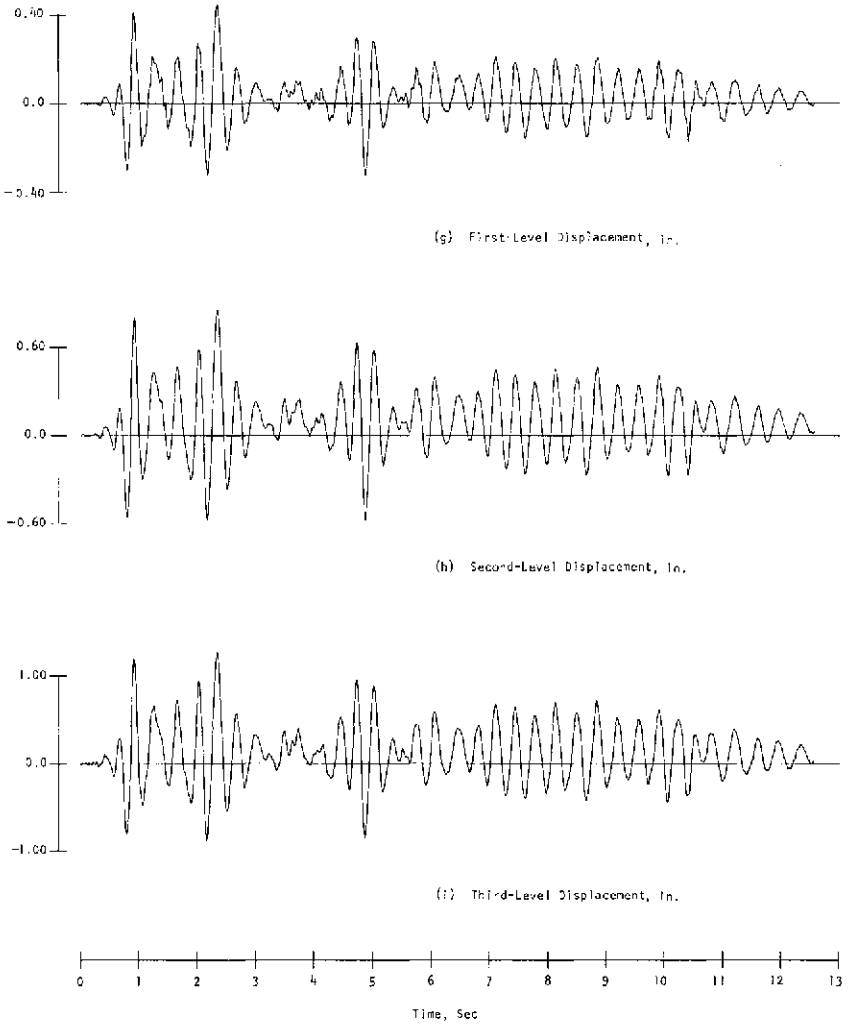

FIG. 8 (Cont'd) TYPICAL OBSERVED RESPONSE (TEST D2-1, BASED ON EL CENTRO 1940 NS, SI_{20} = 15.8 in.)

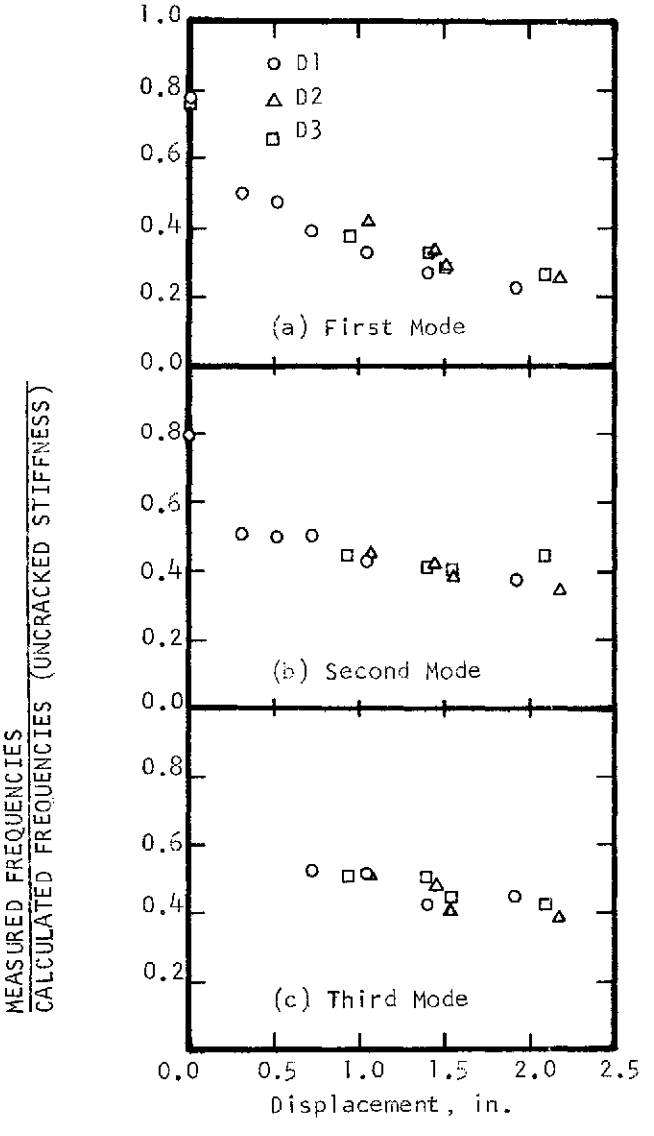

FIG. 9 CHANGE IN FREQUENCIES WITH RESPECT TO ONE-HALF OF THE THIRD-LEVEL DISPLACEMENT RANGE

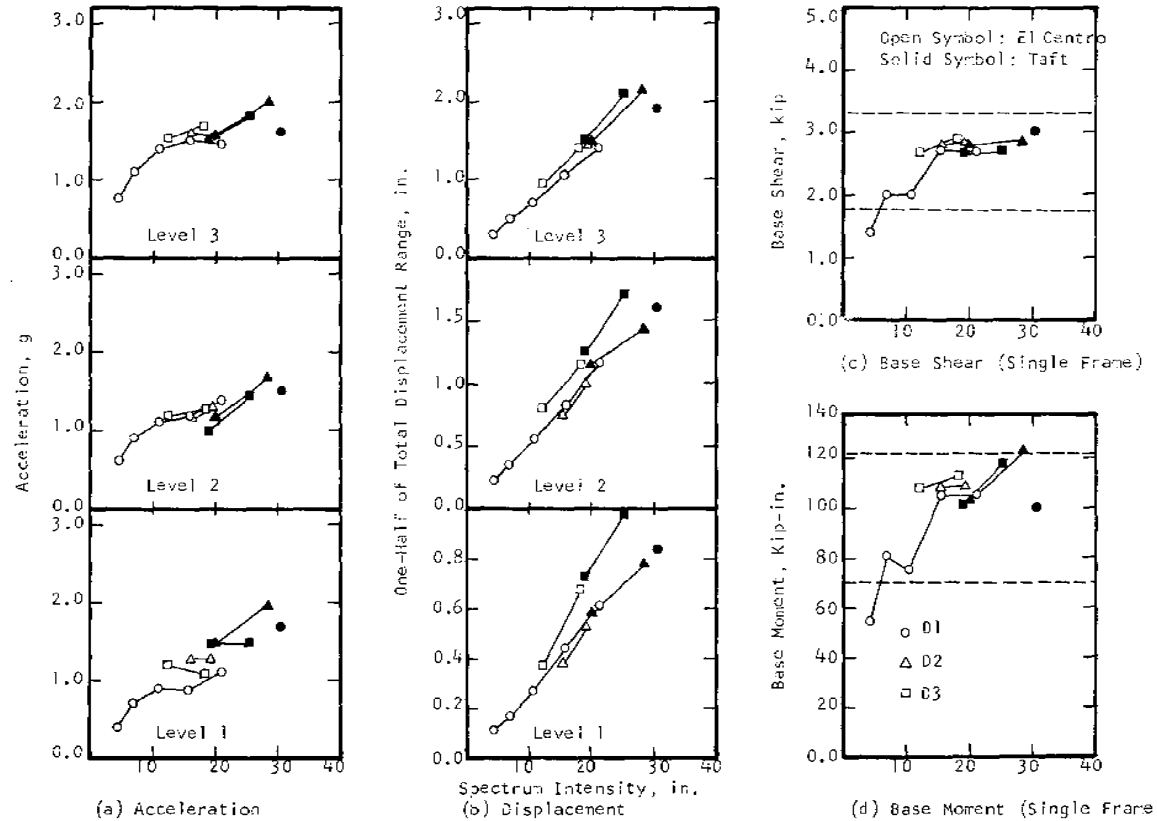

FIG. 10 MEASURED MAXIMUM RESPONSE

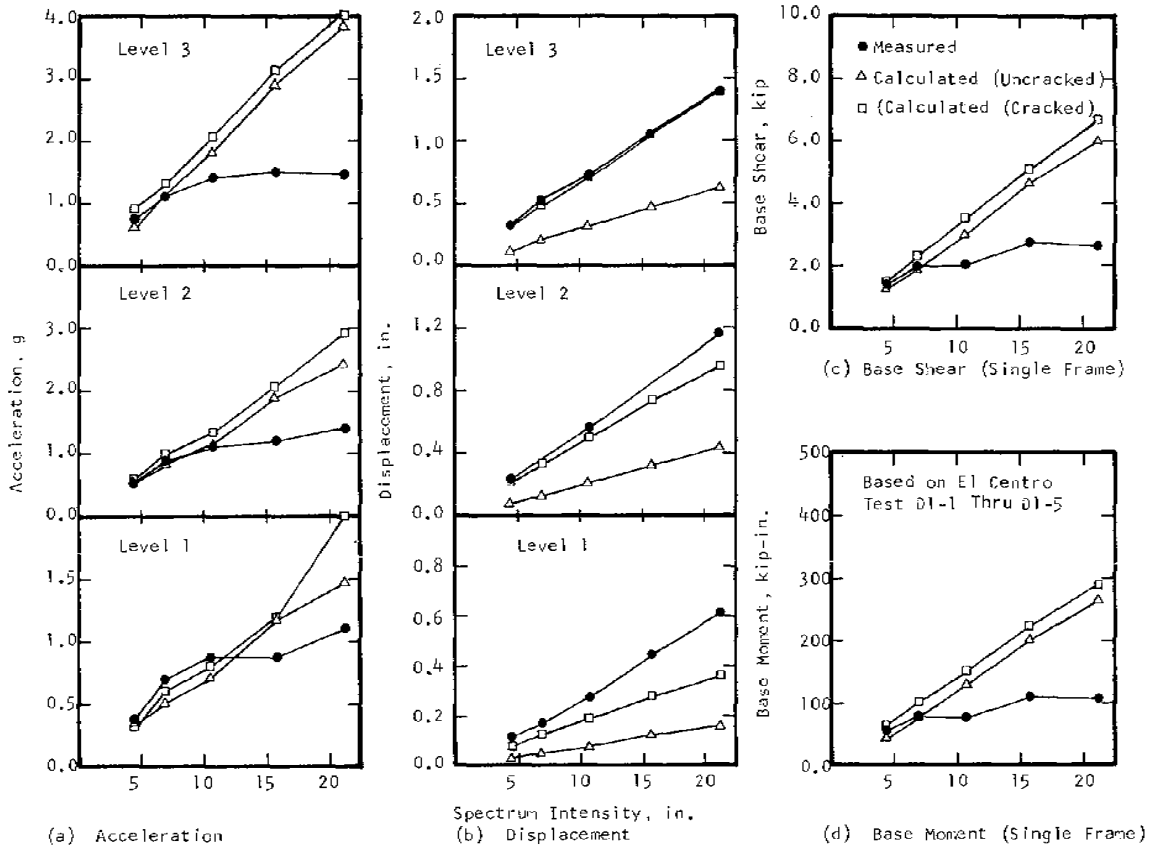

FIG. 11 MEASURED AND CALCULATED (β = 0.05) MAXIMUM RESPONSE

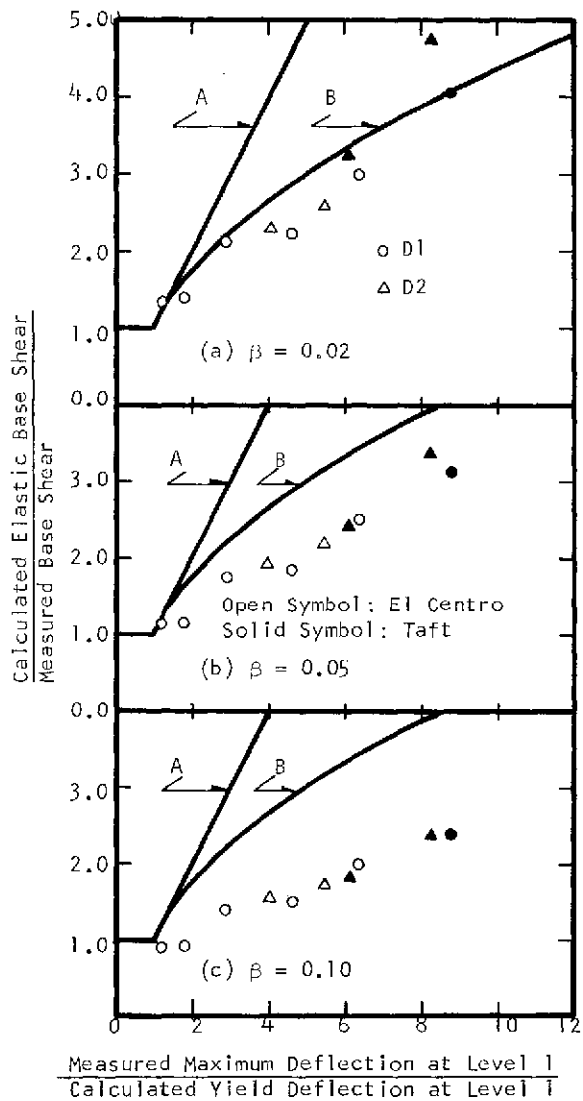

FIG. 12 REDUCTION IN CALCULATED ELASTIC BASE SHEAR AND ATTAINED FIRST-LEVEL DUCTILITY